International Journal of Heat and Mass Transfer 109 (2017) 853–861

Contents lists available at ScienceDirect

International Journal of Heat and Mass Transfer

journal homepage: www.elsevier.com/locate/ijhmt

Spectral emissivity model of steel 309S during the growth of oxide layer at 800–1100 K

Wenjie Zhu, Deheng Shi *, Zunlue Zhu, Jinfeng Sun

College of Physics and Material Science, Henan Normal University, Xinxiang 453007, China

ARTICLE INFO

Article history:
Received 13 September 2016
Received in revised form 18 January 2017
Accepted 21 February 2017
Available online 19 March 2017

Keywords:
Oxide layer
Steel 309S
Temperature measurement
Multispectral radiation thermometry
Spectral emissivity model

ABSTRACT

This work strived to determine the analytical relationships between the spectral emissivity and the wavelength at different temperatures during the growth of oxide layer on the specimen surface of steel 309S. In the experiment, the spectral emissivity was measured at eight wavelengths, 1.4, 1.5, 1.6, 1.7, 1.8, 1.9, 2.0, and 2.1 μm, at temperatures from 800 to 1100 K in increments of 20 K by multispectral radiation thermometry. To accurately measure the normal spectral emissivity, the detector employed in the thermometry should be perpendicular to the surface of specimens as accurately as possible. The temperature of specimen surface was measured by the two thermocouples, which were symmetrically welded onto the front surface of specimens. The average of their readings was regarded as the true temperature. With the spectral emissivity measured here, the variation in the spectral emissivity with wavelength was evaluated at different temperatures and different heating times. Ten emissivity models were evaluated. The effect of number of the parameters used in the models on the fitting accuracy was studied. Both the five-parameter LLWE and LWE models were very suitable for fitting the spectral emissivity and could farthest relieve the effect of heating time on the accuracy of temperature prediction. The uncertainties in the temperature prediction of steel 309S specimens were basically within 10 K by thermometry using the two models over the present temperature and wavelength ranges.

1. Introduction

Radiation thermometry is an indirect technique for measuring a body temperature using radiation emitted from its surface. This technique is very effective for a fast-moving body such as various steels in manufacturing processes. Unfortunately, this technique requires some prior knowledge of spectral emissivity of a body if we want to use it to measure the true temperature accurately [1]. As we know, spectral emissivity may observably vary with wavelength and temperature. More importantly, even if the wavelength and temperature are fixed, emissivity can easily change due to different physical and chemical surface conditions, especially to the surface oxidization of various metals exposed in air at an elevated temperature (i.e., above 800 K for steels in various production processes) for a long time [2]. It is very hard to obtain the accurate spectral emissivity data, which can be directly used in radiation thermometry to accurately evaluate the true temperature in various circumstances [3,4]. That is, to accurately measure the temperature of various steels in production processes by thermometry, we must understand the effect of surface oxidization on the spectral emissivity of steels.

To accurately understand the effect of surface oxidization on the spectral emissivity of various steels, an amount of experimental work [2,4–14] was done in recent years at selected wavelengths and selected temperatures. For example, Kobayashi et al. [2] in 1999 used the radiation thermometry to measure the time variation of normal spectral emissivity of several steels at wavelengths ranging from 0.55 to 5.3 μm over a temperature range from 1053 to 1473 K. Pujana et al. [5] in 2007 employed their precision radiometer to evaluate the spectral emissivity of steels as a function of surface oxidization at wavelengths of 2.12, 4 and 8 μm and at 959 and 1073 K. Cao et al. [6] in 2012 used Fourier Transform Infrared (FTIR) spectrometer to measure the time variation in the spectral emissivity of several steels with wavelength at different oxidization states over an extensive wavelength range at several selected temperatures. Švantner et al. [7] in 2013 measured the spectral emissivity of AISI 1015 steel at 523 K over a wide wavelength range. However, they did not investigate the effect of surface oxidization on the spectral emissivity. Very recently, our group [4,8–11] measured the normal spectral emissivity of several steels at 1.5 μm over a temperature range from 800 to 1100 K. Our group also evaluated the time variation in the normal spectral

* Corresponding author.
E-mail address: scattering@sina.com.cn (D. Shi).

http://dx.doi.org/10.1016/j.ijheatmasstransfer.2017.02.062
0017-9310/

emissivity with surface oxidization during the 6 h heating time at a certain temperature and determined the analytic relationships between the normal spectral emissivity and the heating time. From the experimental work [2,4–6,8–11], we can clearly see that the surface oxidization has great effect on the spectral emissivity. However, all these studies [2,4–6,8–11] did not evaluate any steel emissivity models varying with wavelength and temperature, let alone the effect of surface oxidization on the fitting accuracy of these emissivity models during the growth of oxide layer.

Wen [12] in 2010 used Fast Infrared Array Spectrometer (FIAS) to measure the spectral emissivity of six steels at 700, 800 and 900 K over a wavelength range from 1.2 to 4.8 μm. With these emissivity data, on one hand, Wen [12] investigated the analytical models between the spectral emissivity and the wavelength, temperature and then applied these models to the thermometry so as to infer the steel temperature; on the other hand, Wen studied the effect of heating time on the spectral emissivity, but he did not evaluate the effect of surface oxidization on the fitting accuracy of emissivity models. Wen and Lu [13] in 2010 used the FIAS to measure the spectral emissivity of three types of steels at 700, 800 and 900 K over a wavelength range from 1.2 to 4.8 μm. They [13] used six emissivity models to fit the variation in the emissivity with wavelength and temperature and then applied these models to the thermometry so as to infer the surface temperature of corresponding steels. Wen [14] in 2011 used the FIAS to measure the spectral emissivity of several steels at 700, 800 and 900 K at wavelengths ranging from 1.2 to 4.8 μm. As with their previous work [12,13], Wen [14] first used several types of emissivity models to fit the experimental data and then applied these models to the thermometry to validate their accuracy in the temperature prediction. All these investigations [12–14] examined the analytic relationships between the spectral emissivity and the wavelength, temperature.

Summarizing the results noted above, we find that no experiments reported the effect of surface oxidization on the fitting accuracy of emissivity models till today, though some work in detail studied the effect of heating time on the spectral emissivity [2,4–6,8–12]. In our recent work [4,8–11], we found that the uncertainties in the temperature and normal spectral emissivity of various steels brought about only by the surface oxidization could exceed 10 K and 10%, respectively. Can such surface oxidization of steels generate any observable effect on the accuracy of temperature prediction in thermometry? How can we farthest relieve the effect of surface oxidization on the accuracy of the temperature prediction? To accurately predict the surface temperature of steels by thermometry, we must thoroughly understand the effect of surface oxidization on the fitting accuracy of emissivity models used.

We select steel 309S as the target of this paper. The reason is that no emissivity models of this steel can be available, let alone the effect of surface oxidization on the fitting accuracy of emissivity models. In the next section, we will briefly describe the experimental principle. In Section 3, we will in brief introduce the experimental setup used. In Section 4, we describe the measurement procedure. In Section 5, we report the spectral emissivity over a wavelength range from 1.4 to 2.1 μm at several selected temperatures and evaluate some emissivity models at different heating time for the accuracy of temperature predictions. In Section 6, we give some concluding remarks. It should be noticed that we employ the nomenclature "heating time" to represent the "surface oxidization" in the following descriptions.

2. Experimental principle

The thermometry employed in the experiment had eight wavelengths, which were 1.4, 1.5, 1.6, 1.7, 1.8, 1.9, 2.0 and 2.1 μm, respectively. The bandwidth of each wavelength is approximately 20 nm. The eight wavelengths were obtained by the eight narrow-band interference filters mounted onto the chopper wheel. Each wavelength in thermometry can be regarded as a single-wavelength setup outlined in our earlier papers [4,8–11] when we measured the infrared radiances stemming from the specimen surface. Fig. 1 depicts the schematic diagram of positioning method of two thermocouples, one detector used in thermometry and one piece of specimens. In the experiment, the detector should be perpendicular to the specimen surface as accurately as possible so that we could measure the normal radiances as accurately as possible.

The specimen was heated to a certain temperature by an eddy current heater. The temperature of specimen surface was measured by the two thermocouples, which were symmetrically welded onto the front surface of specimens near the measuring area. The average of their readings was regarded as the true temperature of specimen surface.

Assuming that the ith wavelength of thermometry is λ_i (i = 1, 2, 3, 4, 5, 6, 7 and 8, respectively, corresponding to 1.4, 1.5, 1.6, 1.7, 1.8, 1.9, 2.0 and 2.1 μm) and that the normal radiance received by the detector at λ_i and T is P_i, P_i can be written as [4,8–11]

$$P_i = \frac{\pi^2}{4}\left(\frac{D}{f'}\right)^2 A \int_{\lambda_{i1}}^{\lambda_{i2}} \tau_\lambda \varepsilon(\lambda, T) L_{\lambda,T} d\lambda \tag{1}$$

where T is the temperature of the specimen surface; D and f' are the aperture diameter and the focal length, respectively, of the optical receiving system in the thermometry; A is the area of the sensitive unit of the detector; λ_{i1} and λ_{i2} are the spectral limits of the optical receiving system used to select the spectral bandwidth of the ith wavelength; τ_λ is the total transmissivity of the atmosphere and optical receiving system; and $\varepsilon(\lambda,T)$ is the normal spectral emissivity of specimens at λ and T. Using Planck law, we re-write Eq. (1) as

$$P_i = \frac{\pi^2}{4}\left(\frac{D}{f'}\right)^2 A \int_{\lambda_{i1}}^{\lambda_{i2}} \tau_\lambda \varepsilon(\lambda, T) 2\pi h c^2 \lambda^{-5} \left[\exp\left(\frac{hc}{\lambda kT}\right) - 1\right]^{-1} d\lambda \tag{2}$$

where h is the Planck constant; c is the speed of the light; and k is the Boltzmann constant. The band width $\Delta\lambda$ of each interference filter is approximately 20 nm, which is very narrow. In such a narrow bandwidth, the variation in τ_λ and $\varepsilon(\lambda,T)$ with wavelength at a certain temperature can be neglected. Therefore, we can approximately regard τ_λ and $\varepsilon(\lambda,T)$ as a constant, although τ_λ and $\varepsilon(\lambda,T)$ are never a constant between λ_{i1} and λ_{i2}. With these considerations, Eq. (2) can be simplified as

$$P_i = C_i \cdot \varepsilon(\lambda_i, T)\left[\exp\left(\frac{hc}{\lambda_i kT}\right) - 1\right]^{-1} \tag{3}$$

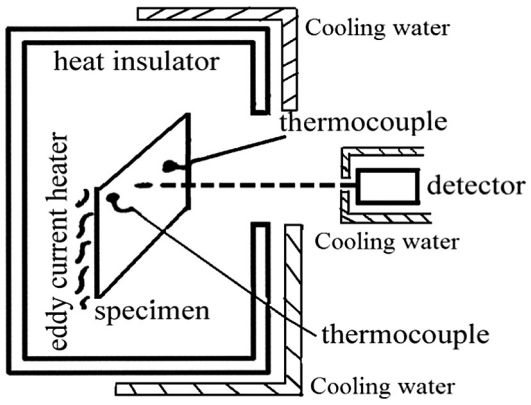

Fig. 1. Schematic diagram of positioning method of thermocouples, detector and specimen.

by setting

$$C_i = \frac{\pi^3}{2}\left(\frac{D}{f'}\right)^2 A\tau_{\lambda_i} hc^2 \lambda_i^{-5}\Delta\lambda \tag{4}$$

In Eq. (4), D, f', A, $\tau_{\lambda i}$, λ_i and $\Delta\lambda$ are the parameters of thermometry. These parameters are all constant for the ith wavelength. That is, C_i is the same for all the specimens and can be accurately evaluated as one of the instrument parameters for each wavelength, only if the configuration of experimental setup does not change. It should be noticed that each C_i would be separately calibrated for each wavelength since the response factors of the InGaAs detector used here at different wavelengths are different. Our earlier papers [8–11] introduced how to calibrate the parameter C_i. Once the parameter C_i is determined, we can use Eq. (3) to accurately measure the normal radiance P_i at a certain temperature.

2.1. How to measure the spectral emissivity at each wavelength

We briefly present how to measure the normal spectral emissivity at each wavelength using multi- spectral radiation thermometry. Assuming that the radiance coming from a blackbody emitter at λ_i and T_0 is $P_{i,0}$, $P_{i,0}$ can be written as

$$P_{i,0} = C_i\left[\exp\left(\frac{hc}{\lambda_i kT_0}\right) - 1\right]^{-1} \tag{5}$$

where T_0 is the surface temperature of specimens measured by the two thermocouples. According to the definition of spectral emissivity, ε_{λ_i} can be written as [8–11]

$$\varepsilon_{\lambda_i} = \frac{P_i}{P_{\lambda_i,0}} \tag{6}$$

With P_i measured by the thermometry and T_0 measured by the thermocouples, we could calculate the spectral emissivity at each wavelength and a certain temperature as well as a certain heating time according to Eqs. (5) and (6). The method how to use Eqs. (5) and (6) to calculate the spectral emissivity at a certain wavelength was introduced in detail in our earlier papers [8–11].

After we obtained the spectral emissivity at eight wavelengths and at a certain heating time and a certain temperature, we could use the least-squares technique to evaluate the relationship between the spectral emissivity and the wavelength. In this work, we employed ten models to fit the spectral emissivity. Comparing the fitting results with the experimental ones, we selected the most favorable models and then applied them to thermometry to validate their accuracy in the temperature prediction.

2.2. How to infer the temperature of specimen surface

We simply introduce how to use Eq. (3) in combination with the least-squares technique and the emissivity models obtained in Section 2.1 to infer the surface temperature of specimens. For the ith wavelength, assuming that the measured radiance stemming from a real specimen surface is $P_{meas,i}$, and that the radiance calculated according to Eq. (3) is $P_{cal,i}$, we can infer the temperature T by minimizing the magnitude of following expression [12–14],

$$\chi^2 = \sum_{i=1}^{8}(P_{meas,i} - P_{cal,i})^2 \tag{7}$$

To calculate $P_{cal,i}$ according to Eq. (3), we must know the expression $\varepsilon(\lambda, T)$. It is the reason why the emissivity model is essential in predicting the surface temperature by thermometry. The main target of this work is to study which emissivity models can farthest relieve the effect of heating time on the accuracy of temperature prediction.

3. Experimental setup

The experimental setup consists of two modules. One is the specimen-heating and temperature- controlling system. The other is the multispectral radiation thermometry. The specimen-heating and temperature-controlling system mainly consists of two platinum-rhodium thermocouples, one piece of specimen, one temperature-controlling assembly and one eddy current heater, etc. Thermometry is mainly composed of one InGaAs photodiode detector, one chopper wheel, one signal-controlling and data-computing system, eight narrow-band interference filters, and so on. Eight pieces of interference filters mounted on the chopper wheel were equally spaced.

The experiments were divided into two stages. The first stage was only to measure the spectral emissivity at different heating times regardless of temperature prediction of any specimens. At this time, the thermometry worked only as one spectral emissivity measurement instrument outlined in our earlier papers [8–11]. The second stage was only to validate the emissivity models for the accuracy of temperature prediction regardless of spectral emissivity measurement. At this stage, the thermometry worked only as a temperature-measurement instrument. With the spectral emissivity measured at the first experimental stage, ten emissivity models were evaluated in detail using a least-squares fitting program. Some favorites were selected and then used at the second experimental stage.

Now we briefly describe the working process of this experimental setup. At each experimental stage, the specimen was heated by the eddy current heater to a given temperature and then kept at that temperature in air for approximately 6 h for measurements. The chopper wheel rotated at a constant speed of 2400 r/min. When the chopper wheel rotated one revolution, the InGaAs detector received eight radiant energies, which corresponded to P_i (i = 1, 2, 3, 4, 5, 6, 7 and 8). The radiances received by the detector were converted into the voltage signals for further processing. In the first stage of this experiment, we determined the spectral emissivity at each wavelength according to the method describing in our earlier papers [4,8–11]. With the help of a least-squares fitting program and the emissivity data measured here, we evaluated ten emissivity models. In the second experimental stage, we used the thermometry and the emissivity models obtained here to infer the surface temperature T of specimens by Eq. (7). In the experiment, the InGaAs photodiode detector should be perpendicular to the specimen surface as accurately as possible. According to the positioning method of thermocouples, detector and specimen shown in Fig. 1, only in this way, the reflection radiation from the specimen surface could be farthest relieved.

In the experiment, we used two thermocouples to measure the temperature of specimen surface. The thermocouples were welded onto the front surface of specimens by point discharge. The welding time was approximately within 5 s. This time is so short that the welding process could not generate any observable oxidization changes of specimen surface. The electromagnetic field generated by the eddy current heater could bring about the effect on the accuracy of thermocouples. To get rid of such effect, we employed a switching set to control the working process of the thermocouples and the eddy current heater. That is, when the eddy current heater was working, the thermocouples did not measure the temperature; and when the two thermocouples measured the temperature, the eddy current heater stopped heating. The two thermocouples were carefully calibrated. Their temperature measurement errors were within 2 K.

All the specimens were fabricated from a piece of cold-rolled steel 309S plate. Each specimen was rectangle in shape with dimensions of approximately 10 cm × 7 cm. The surface of each

specimen was specular and bright. The detector sensed a circular area on the specimen surface with a diameter of about 5 mm. The specimen thickness was approximately 1 mm. The distance from the detector to the surface of specimens was approximately 0.5 m. The surrounding temperature of the InGaAs detector was well stabilized by the cooling water system. In our experiment, the surrounding temperature was approximately 20 °C. In the experiment, each new sample was used for each temperature. And when the measurements were repeated at a temperature, a new sample was also used.

In experiment, the specimen was placed near the slip of the heat insulator. The slip was a circle, which dimension was approximately 10 cm. The specimen was dead against the slip of heat insulator. For this kind of experimental arrangement, no heat reflections can enter the detector. It should be noted that the two thermocouples were welded in the front surface of specimen near the measuring area viewed by the detector. Therefore, the temperature measured by the thermocouples was just the surface temperature of the specimen. Because the dimension of the slip is approximately equal to that of the specimen and the specimen is near the slip, the radiation by the heat insulator can be neglected.

In the experiment, the temperature T_0 of the specimen surface was measured by averaging the readings of the two platinum-rhodium thermocouples. T_0 was regarded as the true temperature of the specimen surface. Comparing T_0 obtained by the thermocouples with T inferred by thermometry, we can validate whether the emissivity model employed to infer the surface temperature of specimens is accurate.

One important thing was how to maintain the specimen at a certain temperature during the whole experimental period. In the experiment, maintaining the specimen temperature at a certain value was accomplished by the temperature-controlling assembly, which was the same as that employed in our previous work [4,8–11]. In detail, the temperature-controlling assembly was mainly composed of a microcomputer-controlled propor tional-integral-derivative device, which used the two thermocouples. The two thermocouples were symmetrically welded onto the front surface of the specimen near the measuring area viewed by the detector. If the temperatures measured by the two thermocouples were close to the given value within the 2 K uncertainty, we thought that the temperature distribution on the specimen surface was homogeneous and invariable. In general, the specimen was heated within 5 min from the room temperature to the required temperature in this experiment. Approximately, we included half of the heating time from the room temperature to the required temperature into the total heating time.

The chopper rotated at a speed of 2400 r/min. that is, the total number of emissivity data we could obtain within one second is 40. In this work, we averaged these 40 experimental emissivity data as the final result during that second. The reasons we could do so were as follows. The surface temperature of specimens should be changed very small within one second because the temperature of specimen surface was well stabilized by the temperature-controlling assembly. In addition, the oxidization status of specimen surface was also changed very little within one second. In other words, we could think that the oxidization status of specimen surface is almost the same within one second.

4. Measurement procedure

At the first stage of this experiment, we measured the spectral emissivity of steel 309S specimens at wavelengths 1.4, 1.5, 1.6, 1.7, 1.8, 1.9, 2.0 and 2.1 μm. The measurements were carried out at 16 temperatures from 800 to 1100 K in increments of 20 K. At each temperature, a new specimen was used. The specimen was heated in air and kept at a certain temperature for approximately 6 h so that the surface condition of specimens could be changed from the start of heating to the fully-saturated oxidization. Only in this way, we could measure the spectral emissivity at various oxidization states. The spectral emissivity was measured within 6 h after the stabilization at the required temperature. It should be noticed that the 6 h heating-duration time included the half time from the room temperature to the required temperature.

Here, we used thermometry instead of FTIR and FIAS to measure the spectral emissivity. The reason was that thermometry used here could also easily measure the accurate spectral emissivity at the same oxidization state, as with FTIR and FIAS. And the response speed of thermometry was also fast enough when the chopper wheel rotated at a high speed. Different from FTIR and FIAS, the sensitivity of InGaAs detector is dependent on the wavelength. That is, its sensitivity is not constant within the present wavelength range. However, we could use the blackbody emitter to perfectly solve this problem by carefully calibrating the detector system at each wavelength.

During the whole experiment, the chopper wheel in thermometry rotated at a constant speed of 2400 r/min. It meant that we could measure 40 radiant values and 40 spectral emissivity data in one second for a certain wavelength. To eliminate the random errors in the experiment and improve the reliability of the measurements, we took the averages of the 40 experimental values measured within one second as the final radiance and the final spectral emissivity at that wavelength for a certain heating time. For example, during the tenth minute one second (from ten min 0 s to ten min 1 s), the averages based on the 40 experimental data were regarded as the radiance and the spectral emissivity at that given heating time, the tenth minute one second, for that wavelength at that temperature.

5. Results and discussion

Once we obtained the spectral emissivity data at eight wavelengths, we could directly evaluate the variation in the spectral emissivity with wavelength at a certain temperature using the least-squares fitting program. For the sake of length limitation, we only take the spectral emissivity measured at 900 and 1060 K as examples for the present discussion. To avoid congestion, we only depict the variation in the spectral emissivity with wavelength for the given heating times, 30, 120, 210 and 300 min, in Fig. 2.

We do not show the variation in the spectral emissivity with heating time at a certain wavelength and a certain temperature due to length limitation. Instead of it, we summarize the main futures of such variation. On one hand, at each wavelength, only one strong oscillation occurred within approximately 20 min from the heating start; on the other hand, the spectral emissivity was rapidly increasing within approximately 200 min from the start of heating. Then the increasing of the spectral emissivity became slower and slower and gradually saturated with the heating duration. These results were very similar with those reported in our previous papers [8–11].

To evaluate whether the random errors in the experiment generate any observable effect on the spectral emissivity, we used another two pieces of steel 309S specimens to carry out the repeating measurements at 1000 and 1100 K. Comparing the variation in the spectral emissivity with heating time between different specimens at each wavelength, we found that the reproducibility of spectral emissivity was excellent. Good reproducibility showed that the random errors in the experiment did not yield any observable effect on the spectral emissivity. It proved that the present experimental setup is reliable.

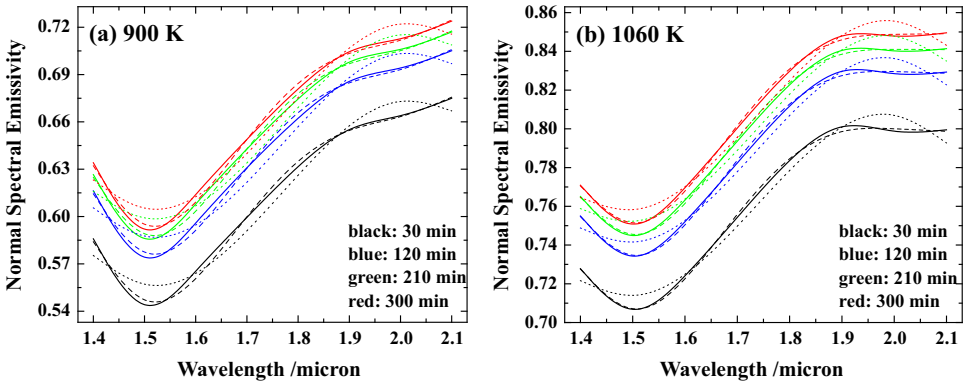

Fig. 2. Curves of spectral emissivity of steel 309S versus wavelength at a certain heating time. Solid line: experimental results; dash line: fitted by LWE model 2-4; dot line, fitted by LWE model 2-3.

Fig. 2 shows one important feature about the variation in the spectral emissivity with wavelength. That is, at different heating times, all the emissivity curves are almost governed by the same trend, which suggests us that we should use the same emissivity model to describe them.

From Fig. 2, we can also clearly confirm that the spectral emissivity increases on the whole as the heating time increases. The effect of heating time on the spectral emissivity is somewhat obvious at a certain wavelength and a certain temperature. The problem discussed here is whether the spectral emissivity data measured at different heating times over the same wavelength range could be really governed by the same rules.

The following discussion is divided into four subsections. The first part is to use the spectral emissivity measured by thermometry to find the most favorable emissivity models. We would fit the spectral emissivity results by ten emissivity models and study the effect of number of the parameters used in the emissivity models on the fitting accuracy. The second part is to evaluate the effect of heating time on the fitting accuracy of emissivity models so that we could determine which model can farthest relieve the effect of heating time on the temperature prediction. The third part is to evaluate the approximation models including the spectral emissivity dependence, wavelength, and temperature at different heating times. And the fourth part is to employ the emissivity models obtained in this paper to infer the surface temperature of specimens by thermometry. Comparing the temperatures measured by the thermocouples with the ones inferred by thermometry, we could instantly evaluate whether the emissivity models obtained here are really suitable for the temperature predictions of steel 309S.

5.1. Models obtained by fitting the experimental spectral emissivity

According to the features demonstrated in Fig. 2, we use ten emissivity models to fit the spectral emissivity data. These models are collected in Table 1. For convenience of discussion, we divide these models into four groups: log-linear wavelength emissivity (LLWE) model, linear wavelength emissivity (LWE) model, log-linear root-wavelength emissivity (LLRWE) model, and log-linear wavelength temperature emissivity (LLWTE) model [12–14].

The evaluation of emissivity models was divided into two steps. The first step was to evaluate the variation in the spectral emissivity with wavelength at different temperatures but at the same heating time, 30 min, so that we could find which type of model was suitable for accurately fitting the data. That is, all the emissivity dada used in this step were measured at the same heating duration time, 30 min, so that we could momentarily dismiss the effect of variation in the surface oxidization on the fitting accuracy of emissivity models. The second step was to study whether the number of parameters used in the models had effect on the fitting accuracy. All the spectral emissivity data used in this step were also measured only at same heating time, 30 min. The main target of this step was to find the most favorable emissivity model. For the sake of length limitation, we only depict the fitting curves obtained by the emissivity models 1-4, 2-4, 3 and 4 at 900 and 1060 K in Fig. 3. For convenience of discussion, we collect the corresponding fitting parameters in Table 2. In Table 2, E_{RMSE} is the root- mean-square error, and R the correlation coefficient obtained in the fitting process.

We first discuss the variation in the spectral emissivity with wavelength at 900 and 1060 K. From Fig. 3, we clearly see that the curves fitted by models 3 and 4 greatly deviate from the experimental ones. From Table 2, we can also see that E_{RMSE} is large and R greatly deviates from 1. That is, the LLRWE and LLWTE models are not suitable for accurately fitting the spectral emissivity of steel 309S. When we fit these models using the spectral emissivity data obtained at other temperatures, we can draw the same conclusion. According to these results, we neglect the two models in the following discussion.

Then we evaluate the fitting accuracy of models 1-4 and 2-4 at 900 and 1060 K. From Fig. 3, we see that the curves fitted by the two models agree well with the corresponding experimental ones.

Table 1
Ten emissivity models examined in this work.

Model	Function	Model	Function
LLWE		LWE	
1-1	$\varepsilon_\lambda = \exp(a_0 + a_1\lambda)$	2-1	$\varepsilon_\lambda = a_0 + a_1\lambda$
1-2	$\varepsilon_\lambda = \exp(a_0 + a_1\lambda + a_2\lambda^2)$	2-2	$\varepsilon_\lambda = a_0 + a_1\lambda + a_2\lambda^2$
1-3	$\varepsilon_\lambda = \exp(a_0 + a_1\lambda + a_2\lambda^2 + a_3\lambda^3)$	2-3	$\varepsilon_\lambda = a_0 + a_1\lambda + a_2\lambda^2 + a_3\lambda^3$
1-4	$\varepsilon_\lambda = \exp(a_0 + a_1\lambda + a_2\lambda^2 + a_3\lambda^3 + a_4\lambda^4)$	2-4	$\varepsilon_\lambda = a_0 + a_1\lambda + a_2\lambda^2 + a_3\lambda^3 + a_4\lambda^4$
LLRWE		LLWTE	
3	$\varepsilon_\lambda = \exp(a_0 + a_1\sqrt{\lambda})$	4	$\varepsilon_\lambda = \exp(a_0\lambda + a_1 T)$

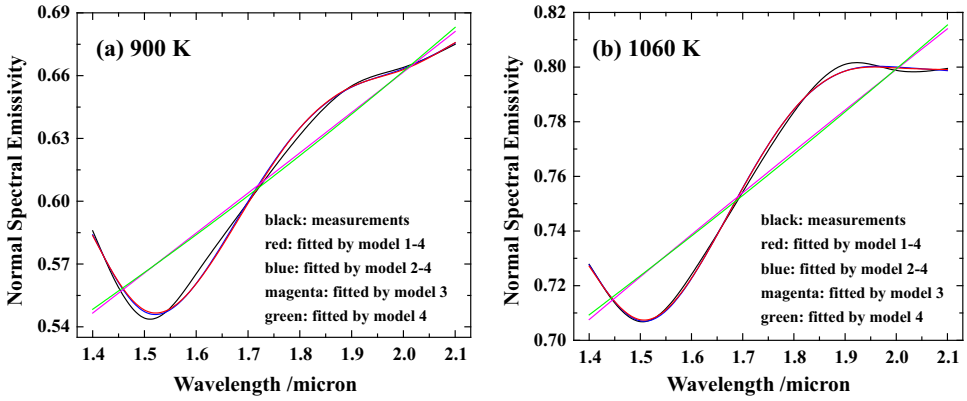

Fig. 3. Comparison of the fitting curves obtained by different emissivity models.

Table 2
Fitting parameters of the emissivity models at temperatures of 900 and 1060 K when the heating time is 30 min from the start of heating.

T/K	Model	a_0	a_1	a_2	a_3	a_4	E_{RMSE}	R
900	1-4	129.7178	−293.9758	246.3648	−90.9610	12.5030	0.0051	0.995
	2-4	75.5966	−169.1716	141.6607	−52.2604	7.1780	0.0047	0.995
	3	−1.5832	0.8275				0.0215	0.898
	4	0.3136	−0.0012				0.0213	0.900
1060	1-4	73.7904	−167.1515	139.7956	−51.4238	7.0310	0.0026	0.998
	2-4	54.5293	−121.1054	101.0583	−37.0826	5.0568	0.0027	0.998
	3	−0.9695	0.5370				0.0168	0.901
	4	0.1991	−0.0006				0.0170	0.899

From Table 2, we find that E_{RMSE} is very small and R is very close to 1. In combination with all the results noted here, we confirm that models 1-4 and 2-4 are very suitable for accurately fitting the spectral emissivity data. When we examine the two models using the spectral emissivity data obtained at other temperatures, we can also derive the same conclusion.

We should notice that LLWE models 1-1, 1-2, 1-3, and 1-4 are the same type. The only difference among them is the number of parameters used. So is it for LWE models 2-1, 2-2, 2-3, and 2-4. Now we study the effect of number of the parameters used in the LLWE and LWE models on their fitting accuracy. We still use the spectral emissivity obtained at the heating duration time, 30 min, for the discussion. Obviously, model 1-1 draws almost a line and model 2-1 gives a strict line. Therefore, we give them up. We have fitted all the spectral emissivity data obtained at each temperature using models 1-2, 1-3, 1-4, 2-2, 2-3, 2-4. For the sake of length limitation, in Fig. 4, we only demonstrate the fitting curves at 900 and 1060 K. For convenience of discussion, we collect the fitting parameters in Table 3.We dismiss the fitting results of models 1-4 and 2-4 from Table 3 because these parameters are collected in Table 2.

From Fig. 4, we can clearly see that the curves fitted by models 2-3 and 2-4 agree favorably with the corresponding experimental ones, and that the curves fitted by model 2-4 are somewhat closer to the experimental ones than those fitted by model 2-3. According to these results, we can confirm that the more the number of the parameters used in the model is, the more the fitting quality becomes. When we examine the spectral emissivity data obtained at other temperatures, we could draw the same conclusion. That is, the five-parameter LWE model can give the best overall fitting results.

As a conclusion, the five-parameter LWE and LLWE models almost give the same fitting quality, and their fitting quality is superior to that of the four-parameter LWE and LLWE models. To avoid the congestion, we do not show the curves fitted by the LLWE models in Fig. 4.

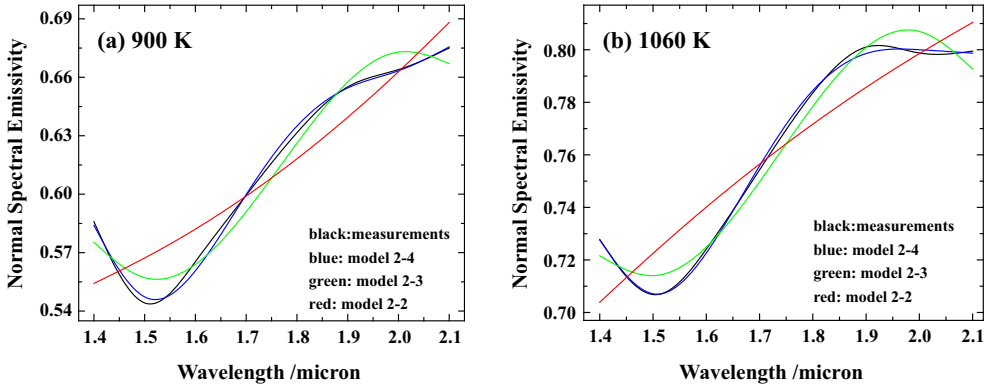

Fig. 4. Comparison between the fitting quality and the number of parameters used in the LWE model.

Table 3
Fitting parameters of the LLWE and LWE models at 900 and 1060 K and at the heating duration time, 30 min.

T/K	Model	a_0	a_1	a_2	a_3	E_{RMSE}	R
900	1-2	−0.7558	−0.0135	0.0926		0.0211	0.901
	1-3	16.1570	−29.4809	17.0292	−3.2125	0.0126	0.966
	2-2	0.6031	−0.1857	0.1077		0.0210	0.903
	2-3	11.0519	−18.4698	10.6620	−2.0104	0.0118	0.970
1060	1-2	−0.9720	0.6036	−0.1150		0.0165	0.905
	1-3	10.3413	−19.138	11.2495	−2.1590	0.0085	0.975
	2-2	0.3156	0.3609	−0.0596		0.0166	0.903
	2-3	9.0726	−14.9628	8.7858	−1.6848	0.0081	0.978

5.2. Effect of heating time on the fitting accuracy of emissivity models

According to the conclusions obtained in Section 5.1, the four- and five-parameter LWE and LLWE models can give the favorite fitting results at the heating time, 30 min. To evaluate how much the heating times bring about the effect on the fitting accuracy of these two models, we also evaluate the variation in the spectral emissivity with wavelength at the heating times, 120, 210 and 300 min, respectively, at temperatures from 800 to 1100 K in increments of 20 K. Due to length limitation, we depict the fitting curves obtained only by LWE model at 900 and 1060 K in Fig. 2 and collect the corresponding fitting parameters in Tables 4 and 5, respectively. In Tables 4 and 5, t represents the heating time from the heating start. Here, we do not collect the fitting results obtained by the four- and five-parameter LWE models at the 30 min heating time in Tables 4 and 5 because these results are presented in Tables 2 and 3.

Now we evaluate the effect of heating time on the fitting accuracy of four-parameter LWE model at 900 and 1060 K. As clearly depicted in Fig. 2, the deviations of fitting curves from their respective experimental ones are almost similar at different heating times, 30, 120, 210 and 300 min. As tabulated in Tables 3 and 4, E_{RMSE} and R are almost constant at different heating times. It shows that the four- parameter LWE model receives little effect of heating time on its fitting accuracy, though the fitting accuracy is somewhat poor. When we examine the emissivity data obtained at other temperatures, we can confirm the same conclusion.

Then we examine the effect of heating time on the fitting accuracy of five-parameter LWE model. As displayed in Fig. 2, the fitting curves obtained by the five-parameter LWE model almost overlap with their respective experimental ones. As collected in Tables 2 and 5, E_{RMSE} is much near 1 and R is very small. These results show that the five-parameter LWE model is an excellent candidate to fit the spectral emissivity obtained at different heating times. That is, the five-parameter LWE model can give the excellent fitting results regardless of heating times. When we examine the spectral emissivity data obtained at other temperatures, we can derive the same conclusion. It suggests us that the effect of heating time on the fitting accuracy of five-parameter LWE model could be ignored over the present temperature and wavelength ranges.

The fitting quality of the four- and five-parameter LLWE models is similar with that of the four- and five-parameter LLE models, respectively. Both the four- and five-parameter LLWE models also receive little effect of heating time on the fitting quality. In addition, the curves fitted by five-parameter LLWE model are slightly closer to the experimental ones than those fitted by the four-parameter LLWE model. For the sake of length limitation, we do not show the fitting curves obtained by the four- and five-parameter LLWE models and do not collect the corresponding fitting parameters here.

According to the above discussion, we think that the five-parameter LLWE and LWE models can give the best fitting quality regardless of heating times. Thus, we use the two models to predict the surface temperature in thermometry in Section 5.4.

Summarizing the results obtained in Sections 5.1 and 5.2, we confirm that the emissivity data of steel 309S obtained at different heating times abide well by the same five-parameter LLWE and LWE models, though the effect of heating time on the spectral emissivity at each wavelength is obvious even at the same temperature. In other words, the five-parameter LLWE and LWE models can farthest relieve the effect of heating time on the accuracy of temperature predictions.

5.3. Approximation models including the spectral emissivity dependence, wavelength, and temperature at different heating times

We tried our best to evaluate the variation of spectral emissivity with wavelength and temperature at different heating times since such an analytic function containing the wavelength and temperature is very useful in practical use. In the fitting process, we employed various models such as exponential function, logarithm function and polynomial function to fit the spectral emissivity. And finally, we found the following functional form of polynomial and exponential combinations,

$$\varepsilon_\lambda = \exp(a_1\lambda + a_2/T) + a_3\lambda + a_4\lambda^2 + a_5\lambda^3 + a_6\lambda^4 \quad (8)$$

was suitable for fitting the spectral emissivity obtained at temperatures from 800 to 1100 K in steps of 20 K over the wavelength range from 1.4 to 2.1 μm. Here, a_1, a_2, a_3, a_4, a_5 and a_6 are the coefficients obtained by fitting, which have been collected in Table 6.

As seen in Table 6, the correlation coefficient R is near 1, and the root-mean-square error E_{RMSE} is small. It shows that equation (8) is basically suitable for fitting the variation of spectral emissivity with wavelength and temperature over the present temperature

Table 4
Fitting parameters of the four-parameter LWE model at different heating times, 120, 210, and 300 min.

T/K	t/min	a_0	a_1	a_2	a_3	E_{RMSE}	R
900	120	11.0751	−18.4680	10.6675	−2.0126	0.0121	0.969
	210	10.9256	−18.2038	10.5247	−1.9871	0.0120	0.970
	300	11.1480	−18.5687	10.7275	−2.0242	0.0122	0.969
1060	120	9.0728	−14.9155	8.7573	−1.6788	0.0079	0.980
	210	8.9059	−14.6068	8.5794	−1.6447	0.0078	0.981
	300	8.9048	−14.5996	8.5769	−1.6442	0.0079	0.981

Table 5
Fitting parameters of the five-parameter LWE model at different heating times.

T/K	t/min	a_0	a_1	a_2	a_3	a_4	E_{RMSE}	R
900	120	77.6258	−173.8656	145.7585	−53.8365	7.4034	0.0048	0.995
	210	76.6846	−171.7528	144.0088	−53.1945	7.3153	0.0047	0.995
	300	78.1584	−175.0396	146.7517	−54.2061	7.4545	0.0048	0.995
1060	120	53.5761	−118.8319	99.0945	−36.3341	4.9508	0.0026	0.998
	210	53.1964	−118.0263	98.4846	−36.1343	4.9271	0.0024	0.998
	300	53.7061	−119.2117	99.5189	−36.5315	4.9839	0.0025	0.998

Table 6
Fitting parameters of Eq. (8) at different heating times.

t/min	a_1	a_2	a_3	a_4	a_5	a_6	E_{RMSE}	R
30	0.4862	−970.0232	5.3506	−9.3282	5.3127	−1.0077	0.0177	0.979
120	0.4792	−969.5993	5.3254	−9.2849	5.2909	−1.0037	0.0172	0.979
210	0.4767	−969.5312	5.2193	−9.1063	5.1923	−0.9855	0.0169	0.980
300	0.4789	−969.3225	5.2733	−9.2045	5.2479	−0.9958	0.0169	0.980

and wavelength range at different heating times. More accurate analytical relationships are in searching process.

5.4. Application of the emissivity model in multispectral radiation thermometry

Using the least-squares technique given by Eq. (7) together with the five-parameter LWE and LLWE models, we can infer the surface temperature of specimens by thermometry. Comparing the temperatures measured by the thermocouples with the results inferred by thermometry at different heating times, we can easily validate whether the heating time has obvious effect on the accuracy of temperature prediction.

The validations were performed at temperatures from 800 to 1100 K in increments of 20 K. The temperature prediction was made once in one second, in which multispectral radiation thermometry measured one mean radiant value. During the experiment, the steel 309S specimen was heated and kept at a certain temperature for 6 h for measurements so that the oxide layer on the surface of specimens could change from little to being almost fully developed. Comparing the temperatures measured by the thermocouples with the ones inferred by thermometry, we affirmed that the differences between them were basically within 10 K during the 6 h heating period. It shows that both the five-parameter LWE and LLWE models are very suitable for accurately predicting the surface temperature of steel 309S regardless of heating time.

6. Conclusions

This work investigated the effect of surface oxidization on the fitting accuracy of the emissivity models at different heating times. Ten emissivity models were examined using the spectral emissivity data measured by thermometry at various oxidization states of specimen surface. Some findings are summarized as follows.

(1) For each specimen, only one strong oscillation happened at each wavelength. The strong peak appeared within approximately 10 min, and the valley bottom occurred within approximately 20 min from the heating start. From then on, the spectral emissivity rapidly became larger with the heating time duration. Approximately after 200 min from the heating start, the increasing of spectral emissivity became slower and slower with the heating time increased. The surface oxidization became gradually full-saturated.

(2) Both the five-parameter LWE and LLWE models could be used to accurately fit the variation in the spectral emissivity with wavelength at 800–1100 K over the present wavelength range.

(3) The effect of heating time on the temperature prediction of steel 309S could be dismissed when we used the five-parameter LWE and LLWE models to predict the surface temperature. The quality of the four-parameter models was slightly poor when we employed them to predict the surface temperature, though the four-parameter models also seemed to relieve the effect of heating time on the accuracy of temperature prediction.

(4) The difference between the temperatures measured by the thermocouples and the ones inferred by thermometry was basically within 10 K during the 6 h heating period when we employed the five- parameter LWE and LLWE models.

As a final conclusion, both the five-parameter LWE and LLWE models can be used to accurately predict the surface temperature of steel 309S. The two models can farthest relieve the effect of heating times on the accuracy of temperature prediction over the present wavelength and temperature ranges.

Acknowledgments

This work was sponsored by the National Natural Science Foundation of China (NSFC) under Grant Nos. 61077073 and 61177092, and the Program for Science and Technology Innovation Talents in Universities of Henan Province in China under Grant No. 2008HASTIT008.

References

[1] P. Coppa, A. Consorti, Normal emissivity of samples surrounded by surfaces at diverse temperatures, Measurement 38 (2005) 124–131.
[2] M. Kobayashi, M. Otsuki, H. Sakate, F. Sakuma, A. Ono, System for measuring the spectral distribution of normal emissivity of metals with direct current heating, Int. J. Thermophys. 20 (1999) 289–298.
[3] T. Iuchi, Modeling of emissivities of metals and their behaviors during the growth of an oxide film, in: D.C. Ripple (Ed.), Temperature: Its Measurement and Control in Science and Technology, AIP Conference of the Proceedings 684, AIP, Melville, NY, vol. 7, 2003, pp. 717–722.
[4] D.H. Shi, F.H. Zou, Z.L. Zhu, J.F. Sun, Modeling the effect of surface oxidation on the normal spectral emissivity of steel 316L at 1.5 μm over the temperatures ranging from 800 to 1100 K in air, IR. Phys. Technol. 71 (2015) 370–377.
[5] J. Pujana, L. del Campo, R.B. Pérez-Sáez, M.J. Tello, I. Gallego, P.J. Arrazola, Radiation thermometry applied to temperature measurement in the cutting process, Meas. Sci. Technol. 18 (2007) 3409–3416.

[6] G. Cao, S.J. Weber, S.O. Martin, M.H. Anderson, K. Sridharan, T.R. Allen, Spectral emissivity measurements of candidate materials for very high temperature reactors, Nucl. Eng. Des. 251 (2012) 78–83.
[7] M. Švantner, P. Vacikova, M. Honner, Non-contact charge temperature measurement on industrial continuous furnaces and steel charge emissivity analysis, IR. Phys. Technol. 61 (2013) 20–26.
[8] D.H. Shi, Y.W. Pan, Z.L. Zhu, J.F. Sun, Effect on the spectral emissivity of SPHC steel by surface oxidization, Int. J. Thermophys. 34 (2013) 1100–1109.
[9] D.H. Shi, F.H. Zou, S. Wang, Z.L. Zhu, J.F. Sun, Effect of surface oxidization on the spectral emissivity of steel 304 at the elevated temperature in air, IR. Phys. Technol. 66 (2014) 6–12.
[10] D.H. Shi, F.H. Zou, S. Wang, Z.L. Zhu, J.F. Sun, Spectral emissivity modeling of steel 201 during the growth of oxidation film over the temperature range from 800 to 1100 K in air, IR. Phys. Technol. 67 (2014) 42–48.
[11] D.H. Shi, F.H. Zou, Z.L. Zhu, J.F. Sun, Effect of surface oxidization on the normal spectral emissivity of straight carbon steel at 800–1100 K in air, ISIJ Int. 55 (2015) 697–705.
[12] C.-D. Wen, Investigation of steel emissivity behaviors: Examination of multispectral radiation thermometry (MRT) emissivity models, Int. J. Heat Mass Transf. 53 (2010) 2035–2043.
[13] C.-D. Wen, C.-T. Lu, Suitability of multispectral radiation thermometry emissivity models for predicting steel surface temperature, J. Thermophys. Heat Transf. 24 (2010) 662–665.
[14] C.-D Wen, Study of steel emissivity characteristics and application of multispectral radiation thermometry (MRT), J. Mater. Eng. Perform. 20 (2011) 289–297.